

Spatial Distribution and Risk Assessment of Heavy Metals in Urban Road Dust From Shenyang, a Heavy Industrial City in Northeast China

Zhengwu Cui (✉ cuizhengwu@iga.ac.cn)

Northeast Institute of Geography and Agroecology Chinese Academy of Sciences

<https://orcid.org/0000-0002-4260-1002>

Yang Wang

Northeast Institute of Geography and Agroecology Chinese Academy of Sciences

Rui Yu

Northeast Institute of Geography and Agroecology Chinese Academy of Sciences

Yong Yu

Northeast Institute of Geography and Agroecology Chinese Academy of Sciences

Nana Luo

Northeast Institute of Geography and Agroecology Chinese Academy of Sciences

Research Article

Keywords: road dust, heavy metals, pollution level, source identification, health risk

Posted Date: November 12th, 2021

DOI: <https://doi.org/10.21203/rs.3.rs-1051814/v1>

License:  This work is licensed under a Creative Commons Attribution 4.0 International License.

[Read Full License](#)

1 **Spatial distribution and risk assessment of heavy metals in urban road dust from Shenyang, a**
2 **heavy industrial city in Northeast China**

3 Zhengwu Cui^{1,2}, Yang Wang^{1*}, Rui Yu¹, Yong Yu¹, Nana Luo^{1,2}

4 1 Key Laboratory of Wetland Ecology and Environment, Northeast Institute of Geography and
5 Agroecology, Chinese Academy of Sciences, Changchun, China

6 2 University of Chinese Academy of Sciences, Beijing 100049, PR China

7 Corresponding author: Yang Wang. E-mail: wangyangw@iga.ac.cn

8
9 **Abstract:** 124 road dust samples were collected from an urban area of Shenyang, a typical heavily
10 industrial city in Northeast China, to study the concentration, pollution level, source, spatial distribution,
11 and health risk of heavy metals. The average concentrations of Cd, Cr, Cu, Mn, Ni, Pb, and Zn were
12 1.802, 132.1, 60.33, 778.3, 54.80, 86.73, and 391.2 mg/kg, respectively. The levels of metal pollution
13 ranged from minimal to extremely high, with average levels in the ranked order: Mn < Ni < Cr < Cu <
14 Pb < Zn < Cd, indicating that the road dust was heavily polluted by Cd, Zn, and Pb. Source identification
15 results demonstrated that Cr, Mn, and Ni had mixed sources including industrial emissions and
16 weathering of soil, pavements, and building materials, while Cu, Pb, and Zn mainly originated from
17 traffic and industrial activities, and Cd had a complex mixture of sources (with various anthropogenic
18 sources). Hotspots of heavy metal pollution levels were closely correlated with local anthropogenic
19 activities, such as industrial discharge, traffic-related exhaust emissions, and agricultural activities.
20 Furthermore, health risk assessment revealed significant non-carcinogenic risks for children from
21 multiple metals, and the carcinogenic risk assessment identified significant risks for children from Cd,
22 with ingestion being the main exposure pathway for carcinogenic and non-carcinogenic risk for adults
23 and children. However, no health risk was observed due to dermal and inhalation exposure pathways.

24 **Keywords:** road dust, heavy metals, pollution level, source identification, health risk

25
26 **1 Introduction**

27 As a result of rapid global urbanization and industrialization in the last few decades, urban
28 environmental pollution has received widespread attention (Talbi et al. 2017; Yan et al. 2018). Road dust
29 has been found to be an important environmental media, as it can serve as a bond linking various urban
30 environmental issues, in air, water, and soil phases (Lu et al. 2017a; Lu et al. 2017b). Road dust mainly
31 comes from the weathering of exposed soil, as well as anthropogenic activities, including the deposition
32 of atmospheric particulates, vehicle emissions, wear of vehicle brakes and tires, abrasion of building
33 materials and pavements, coal combustion, residential heating, and municipal activities (Li et al. 2016;
34 Ali et al. 2017; Tang et al. 2017; Men et al. 2018b). As an environmental medium, road dust typically
35 adsorbs high concentrations of toxic substances (e.g., heavy metals, polycyclic aromatic hydrocarbons,
36 and polychlorinated biphenyl) (Soltani et al. 2015; Khanal et al. 2018; Anh et al. 2019). Heavy metals
37 are considered to be one of the major environmental pollutants in urban areas, due to their characteristics
38 of high toxicity, non-biodegradability, and bioavailability (Lanzerstorfer 2018; Men et al. 2018a).
39 Therefore, heavy metal contamination of urban road dust and the adverse effects on both environmental
40 and human health, have caused increasing levels of concern (Dehghani et al. 2017; Bi et al. 2018).

41 In recent decades, a series of studies have been conducted on the spatial distribution, source,
42 accumulation, and health risk of heavy metals in road dust (Lu et al. 2010; Wei et al. 2015; Khademi et
43 al. 2018). However, most of these studies have focused on developed countries or megacities (Mathur et
44 al. 2016; Dehghani et al. 2017). In China, heavy metal contamination of road dust has been extensively

45 studied in megacities, such as Beijing (Men et al. 2018b), Shanghai (Bi et al. 2018), Xi'an (Pan et al.
46 2017), and Nanjing (Liu et al. 2014). Urban road dust has also been found to be polluted with heavy
47 metals in many other smaller cities in China, such as Guangzhou (Cai et al. 2013), Tianjin (Hu et al.
48 2016), and Hefei (Ali et al., 2017). However, these studies have largely covered the central and eastern
49 coastal areas of China, which are not typically dominated by heavy industry and it remains unclear
50 whether heavily industrial cities, especially in Northeast China, have a higher degree of heavy metal
51 pollution in road dust.

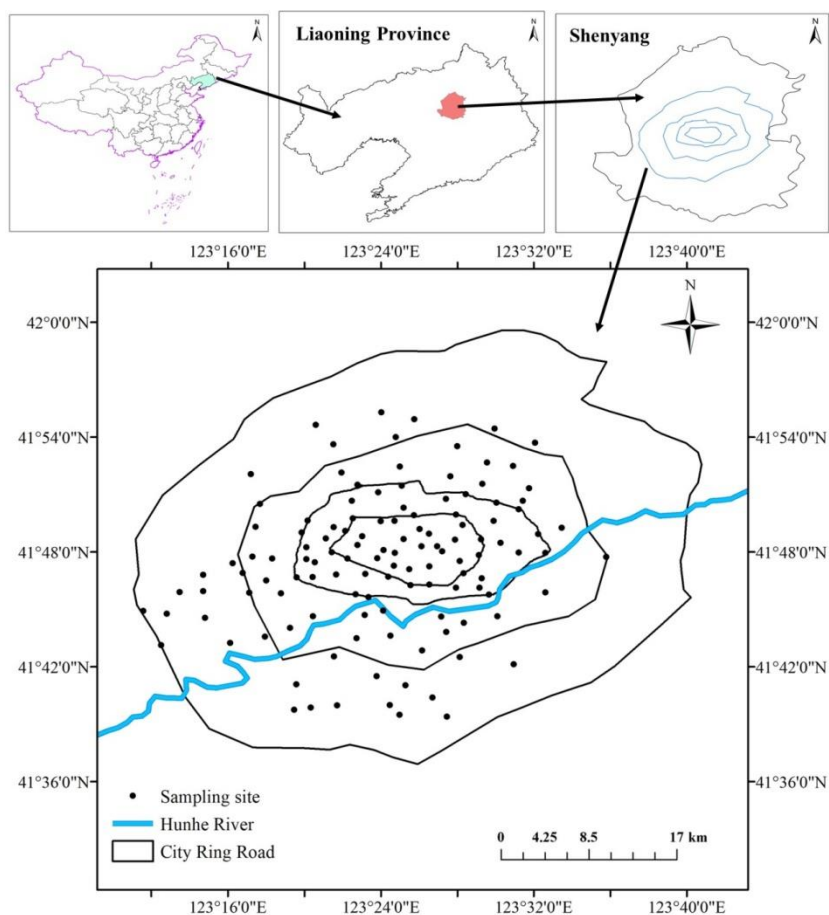
52 Shenyang is an old industrial city in Northeast China and the administrative center of Liaoning
53 Province. Rapid urbanization and industrialization have occurred in Shenyang under the implementation
54 of China's Northeast Revival Strategy. According to the Shenyang statistical yearbook 2010 to 2020, the
55 urban area in 2019 was approximately 1.5-fold greater than in 2010 (SSB, 2020). Shenyang is a crucial
56 industrial hub with equipment manufacturing being the major industry in the area. Large industrial
57 companies, such as the North Heavy Industry Group Co., Ltd. (NHI), SANY Heavy Industry Co., Ltd.,
58 and AVIC Shenyang Aircraft Industry (Group) Co., Ltd., are located in this area. Although the number
59 of industrial enterprises in Shenyang has significantly decreased in the last few years, the potentially high
60 level of historical pollutant residues in this region should not be ignored. As of 2019, the number of motor
61 vehicles of Shenyang had exceeded 2.5 million. Vehicle exhaust emissions and the wear of tires and
62 brakes have resulted in the accumulation of heavy metals in urban road dust. Continuous land demand
63 for city expansion, industrial production for economic development and the increasing volume of motor
64 vehicles in urban areas can increase the accumulation of heavy metals in road dust. Previous studies have
65 reported that heavy metal pollution is widely distributed in urban soil from the Tiexi industrial district of
66 Shenyang (Li et al., 2013; Jiao et al., 2015). However, quantitative information about the accumulation,
67 source, distribution, and health risks of heavy metals in road dust from the main urban areas remains
68 limited. The primary aims of the present study were: 1) to investigate the heavy metals concentrations
69 and distribution in road dust from Shenyang city; 2) to evaluate the heavy metal pollution level; 3) to
70 identify the potential sources of different heavy metals; 4) to assess the potential health risk associated
71 with exposure to these heavy metals, for children and adults via different exposure pathways. The results
72 of this study provide an important multidisciplinary assessment of heavy metals in the urban environment
73 of heavy industrial cities, providing useful guidance for the improvement and development of risk
74 management measures in this region.

75

76 **2. Materials and methods**

77 **2.1. Study area**

78 Shenyang (122°25'-123°48' E, 41°12'-43°20' N) is the capital of Liaoning province and is one of
79 the largest cities in Northeast China, with an urban area of 5116 km² and an estimated population of 8.32
80 million. Shenyang is also one of the most important heavy industry cities in China. At the end of 2019,
81 the number of industrial enterprises in Shenyang was 1579, among which heavy industrial enterprises
82 accounted for 1107. Furthermore, the number of motor vehicles in the city had reached >2.5 million,
83 exhibiting a 2.5-fold increase compared to 2000 (SSB, 2020). The rapid increase in the urban population
84 and the intensity of anthropogenic activities in Shenyang have seriously affected the environmental
85 quality in the region and may pose a health risk to the residents of Shenyang.



86
87 **Fig. 1.** Study area and the sampling locations of dust in Shenyang

88 **2.2 Sampling and chemical analysis**

89 A total of 124 dust samples were collected from the urban area of Shenyang in December 2018 after
 90 one week of continuous sunny weather (Figure. 1). The sampling sites were uniformly distributed across
 91 the main urban area of Shenyang city, with the latitude and longitude of the sampling sites recorded along
 92 with the surrounding environmental conditions. At each sampling site, four to eight sub-samples were
 93 collected from both road and pavement edges at the main street intersection and mixed thoroughly to
 94 obtain a representative bulk sample. For each sub-sample, 500-1000 g of dust was collected by slowly
 95 sweeping dust using a plastic brush and dustpan, directly transferring the dust into plastic bags, which
 96 were labeled and transported to the laboratory for analysis. Extraneous matter, such as cigarette butts,
 97 small stones, plastic waste, metal scraps, and other impurities, was manually removed from the sampling
 98 area prior to dust collection.

99 After the dust samples were air-dried at ambient temperature in the laboratory, they were sieved
 100 through a 53 μm nylon sieve. Previous studies have reported that human exposure to dust particles
 101 smaller than 53 μm in diameter can occur easily via ingestion, inhalation, or dermal absorption (Gope et
 102 al., 2018; Shi and Lu 2018). Therefore, fine particles <53 μm were selected for analysis in the present
 103 study. All dust samples were digested using the $\text{HNO}_3\text{-HClO}_4\text{-HF}$ method (SEPA, 1997) for extraction
 104 of the metals Cd, Cr, Cu, Mn, Ni, Pb, and Zn. The concentrations of Cr, Cu, Mn, Ni, Pb, and Zn in extracts
 105 were measured by flame (air-acetylene) atomic absorption spectrophotometry (FAAS; AA-6300C,
 106 Shimadzu, Japan), while Cd concentrations were determined using a graphite furnace atomizer (GFA;
 107 AA-6300C, Shimadzu, Japan).

108 **2.3 Heavy metal pollution assessment**

109 The geo-accumulation index (I_{geo}), pollution index (PI), and pollution load index (PLI) have been
 110 widely used to assess heavy metal pollution levels (Urrutia-Goyes et al., 2018). The I_{geo} and PI are the
 111 most commonly applied indices used to evaluate single element pollution levels, while PLI has been
 112 widely applied for the assessment of multiple element pollution levels.

113 I_{geo} values were calculated using Equation (1) as follows:

$$114 \quad I_{geo} = \log_2 \left(\frac{C_n}{1.5B_n} \right) \quad (1)$$

115 where, n indicates the heavy metal element; C_n is the heavy metal (n) concentration; and B_n is the soil
 116 background concentration of the heavy metal, applied as 0.108 mg·kg⁻¹ Cd, 57.9 mg·kg⁻¹ Cr, 19.8 mg·kg⁻¹
 117 ¹ Cu, 564 mg·kg⁻¹ Mn, 25.6 mg·kg⁻¹ Ni, 21.1 mg·kg⁻¹ Pb and 63.5 mg·kg⁻¹ Zn, respectively (CNEMC,
 118 1990). The pollution degree was categorized as follows: $I_{geo} \leq 0$, non-polluted; $0 < I_{geo} \leq 1$, light-moderate
 119 pollution; $1 < I_{geo} \leq 2$, moderate pollution; $2 < I_{geo} \leq 3$, moderate-heavy pollution; $3 < I_{geo} \leq 4$, heavy pollution;
 120 $4 < I_{geo} \leq 5$, heavy-extreme pollution; $I_{geo} > 5$, extreme pollution.

121 The PI and PLI were calculated according to Eqs. (2) and (3) as follow (Maanan et al., 2015):

$$122 \quad PI = C_n / B_n \quad (2)$$

$$123 \quad PLI = \sqrt[n]{PI_1 \times PI_2 \times PI_3 \times \dots \times PI_n} \quad (3)$$

124 where, PI represents the single pollution indices. The PI classification was categorized as follows: $PI < 1$,
 125 low contamination; 1-3, moderate contamination; 3-6, considerable contamination; and $PI > 6$, very high
 126 contamination. The PLI was classified as follows: $PLI \leq 1$, low pollution; $1 < PLI \leq 2$, moderate pollution;
 127 $2 < PLI \leq 5$, high pollution; $PLI > 5$, extremely high pollution (Gope et al., 2017).

128 2.4 Health risk assessment

129 The hazard quotient (HQ) and cancer risk (CR) were used to quantitatively establish the non-
 130 carcinogenic and carcinogenic risks presented by heavy metals exposure, respectively. Three exposure
 131 pathways were considered, including direct ingestion, dermal absorption, and inhalation (Gope et al.,
 132 2018). According to the Exposure Factors Handbook (USEPA, 1997), the average daily dose (ADD)
 133 ((mg·kg⁻¹)·day⁻¹) of an element via dust ingestion, dermal contact, and inhalation exposure pathways,
 134 can be estimated using Eqs. (4), (5), and (6) as follow:

$$135 \quad ADD_{ing} = \frac{c_n \times IngR \times EF \times ED}{BW \times AT} \times CF \quad (4)$$

136 where, $IngR$ indicates the dust ingestion rate (mg·day⁻¹); EF is the exposure frequency (days·year⁻¹); ED
 137 is the exposure duration (years); BW refers to the average body weight (kg); AT indicates the averaging
 138 time (days); and CF is the conversion factor (1×10^{-6} kg·mg⁻¹).

$$139 \quad ADD_{der} = \frac{c_n \times SA \times AF \times ABS \times EF \times ED}{BW \times AT} \times CF \quad (5)$$

140 where, SA represents the surface area of skin in contact with the dust (cm²); AF is the skin adherence
 141 factor for dust (mg·(cm²)⁻¹); and ABS is the dermal absorption factor (chemical specific).

$$142 \quad ADD_{inh} = \frac{c_n \times InhR \times EF \times ED}{PEF \times BW \times AT} \quad (6)$$

143 where, InhR indicates the inhalation rate ($\text{m}^3 \cdot \text{day}^{-1}$); and PEF is the particle emission factor, 1.36×10^9
144 $\text{m}^3 \cdot \text{kg}^{-1}$.

145 The potential non-carcinogenic and carcinogenic risks for individual metals were calculated using
146 Eqs. (7), (8), and (9) (US.EPA, 1989), as follow:

$$147 \quad HQ = \frac{ADD}{RfD} \quad (7)$$

$$148 \quad HI = \sum HQ_i \quad (8)$$

$$149 \quad CR = \sum ADD_i \times SF_i \quad (9)$$

150 where, RfD indicates the reference dose ($\text{mg}/(\text{kg} \cdot \text{d})$); and SF is the slope factor (per ($\text{mg}/(\text{kg} \cdot \text{d})$)). The
151 hazard index (HI) is equal to the sum of HQ, where HI values >1 indicate that non-carcinogenic effects
152 may occur, while values <1 indicate no risk of non-carcinogenic effects (USEPA, 2001). CR
153 values $>1 \times 10^{-4}$ indicate an unacceptable health risk, while CR values $<1 \times 10^{-6}$ are not considered to result
154 in significant health effects, with risks generally regarded as tolerable in the CR value range of 10^{-6} - 10^{-4}
155 (Chen et al., 2015; Li et al., 2017). Detailed information on the probabilistic parameters is provided in
156 Table S1 (supplementary materials).

157 **2.5 Quality assurance and quality control (QA/QC)**

158 Reagent blanks and analytical duplicates were used to ensure the accuracy and precision of analysis.
159 Glassware was soaked overnight with HNO_3 (10% v/v) and rinsed thoroughly with deionized water prior
160 to use. A standard reference material (GBW 07405 [GSS-5]) was obtained from the Center of National
161 Standard Reference Material of China, for digestion and determination as part of the quality assurance
162 (QA) protocol. The detected values of Cd, Cr, Cu, Mn, Ni, Pb, and Zn in the reference material were
163 within their certified concentration ranges. The recovery rates for the seven observed metals ranged from
164 90%-110%. The limits of determination (LOD) ($\text{mg} \cdot \text{kg}^{-1}$) of Cd, Cr, Cu, Mn, Ni, Pb, and Zn were 0.001,
165 0.01, 0.1, 0.2, 0.1, 0.01, and 0.1, respectively.

166 **2.6 Statistical analysis**

167 Statistical analysis was performed using SPSS v.16.0 and Excel 2016. Spatial analysis was
168 performed using GIS software to graphically and digitally present the distribution of metals. Heavy metal
169 distribution maps were created using ArcGIS v.9.0. Principal component analysis (PCA) was carried out
170 to cluster metals for the identification of potential sources (Pan et al., 2017). Varimax orthogonal rotation
171 was applied to minimize the number of variables with high loading in each component and facilitate the
172 interpretation of results. Heavy metals with the proportion of variance in <0.5 measurements explained
173 by the extracted components (communality values) were excluded from PCA. In this study, all data were
174 log-transformed prior to PCA to reduce the influence of high values.

175

176 **3. Results and discussion**

177 **3.1. Heavy metal concentrations**

178 Descriptive statistics for the analyzed heavy metal concentrations are listed in Table 1. The
179 background values of Liaoning topsoil (CNEMC, 1990) were applied as reference values. The mean
180 concentrations of Cd, Cr, Cu, Mn, Ni, Pb, and Zn were 1.802, 132.1, 60.33, 778.3, 54.80, 86.73, and
181 $391.2 \text{ mg} \cdot \text{kg}^{-1}$, respectively. Compared to the soil background values, the concentrations of heavy metals
182 in road dust all exhibited elevated concentrations. The mean concentrations of Cd, Zn, Pb, and Cu were

183 16.7-, 6.16-, 4.11-, and 3.05-fold greater than their respective background values, as well as being
 184 significantly higher than the other metals. Conversely, Mn, Ni, and Cr were not enriched as compared to
 185 their respective background values. Similar results have been reported in several previous studies
 186 conducted in China (Li et al., 2017), suggesting that Mn, Ni, and Cr might originate from natural sources,
 187 while other metals present in road dust could originate from anthropogenic activities (Liu et al., 2014).
 188 As a historically industrial city in Northeast China, different kinds of industrial activities occur in
 189 Shenyang, such as engineering and equipment manufacturing, electroplating and the production of
 190 electronics, rubber, pharmaceuticals, textiles, and electric batteries, contributing to Cd, Cu, Pb, and Zn
 191 concentrations. As major components of petroleum and lubricants, heavy metals can be released into the
 192 atmosphere during combustion (Dao et al., 2010), with the deposition of particles from industrial and
 193 vehicle exhaust emissions leading to excessive concentrations of Cd, Cu, Pb, and Zn in road dust
 194 (Trujillo-González et al., 2016).

195 **Table 1** Descriptive statistics for heavy metal concentrations ($\text{mg}\cdot\text{kg}^{-1}$) in road dust samples from
 196 Shenyang

	Mean	Min	Median	Max	SD	CV	Skewness	Kurtosis	Reference value ^a
Cd	1.802	0.010	1.342	7.440	1.407	78.07%	1.818	3.245	0.108
Cr	132.1	41.96	130.9	263.5	43.90	33.23%	0.163	0.039	57.90
Cu	60.33	0.110	58.21	215.9	33.70	55.85%	1.566	4.657	19.80
Mn	778.3	412.9	739.0	5193	425.8	54.72%	9.221	95.62	564.0
Ni	54.80	22.47	47.14	531.1	46.56	84.97%	8.898	90.50	25.60
Pb	86.73	23.65	80.56	411.7	42.19	48.65%	4.126	28.88	21.10
Zn	391.2	176.2	375.8	1446	145.1	37.08%	3.471	22.00	63.50

197 **a** Background values for Shenyang topsoil. (CNEMC, 1990)

198 Table S2 summarizes the concentrations of heavy metals in road dust from different cities in China
 199 and worldwide. Results show that within China, the concentrations of most metals in Shenyang road dust
 200 were higher than in Beijing (Men et al., 2018b) and Xi'an (Shi and Lu, 2018), but lower than Shanghai
 201 (Bi et al., 2018), Nanjing (Li et al., 2013) and Shijiazhuang (Wan et al., 2016). Furthermore, the
 202 concentrations of most metals were lower than the levels detected in Hyderabad (India) (Mathur et al.,
 203 2016) and Toronto (Canada) (Nazzal et al., 2013). Moreover, the concentrations of heavy metals such as
 204 Cu and Pb were lower than those previously reported for Xiangyang (China), Tehran (Iran), and
 205 Kurdistan (Iraq) (Shi et al., 2013; Dehghani et al., 2017; Amjadian et al., 2018). The concentrations of
 206 Cd, Cr, Mn, and Zn were higher than those detected in the road dust from most cities, while Ni
 207 concentrations were not significantly different from those reported for other cities. In general, the metal
 208 concentrations in road dust in the present study were relatively moderate compared with the
 209 concentrations reported for other cities.

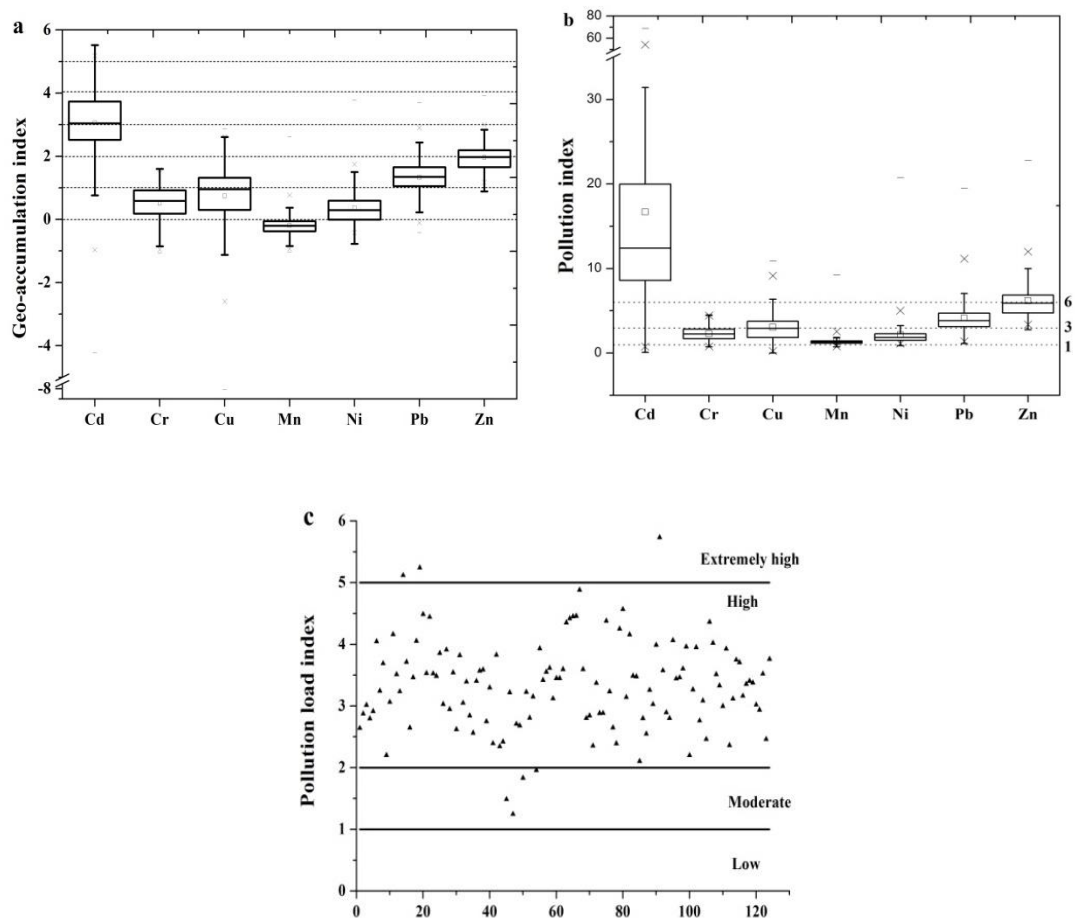
210 3.2. Pollution indices

211 To further characterize the heavy metal pollution level in dust, I_{geo} , PI, and PLI values were
 212 calculated (Fig. 2 and Table S3). The I_{geo} values ranged from -4.22 to 5.22 for Cd (mean 3.06), -1.05 to
 213 1.60 for Cr (mean 0.51), -8.04 to 2.86 for Cu (mean 0.75), -1.04 to 2.62 for Mn (mean -0.19), -0.77 to
 214 3.79 for Ni (mean 0.36), -0.42 to 3.70 for Pb (mean 1.33) and 0.89 to 3.92 for Zn (mean 1.97). The mean
 215 I_{geo} values were ranked in the decreasing order of Cd > Zn > Pb > Cu > Cr > Ni > Mn (Fig. 2a). The
 216 mean I_{geo} for Cd pollution indicated heavily polluted conditions, while Zn and Pb pollution was moderate.
 217 Meanwhile, the mean I_{geo} values obtained for Cu, Cr, and Ni indicated light to moderate pollution

218 conditions, while urban dust exhibited almost no Mn pollution. Table S3 presents the heavy metal
219 contamination distribution characteristics. For Cd, Zn, and Pb, about 96.0%, 99.2%, and 77.4% of all
220 dust samples, respectively, exhibited moderate pollution levels or greater. Therefore, Cd, Zn, and Pb were
221 the primary contributors to contamination in urban road dust from Shenyang.

222 PI values calculated according to the local soil background values varied significantly for different
223 metals (Fig. 2b and Table S3). The mean PI values for all metals were ranked in the descending order of
224 Cd > Zn > Pb > Cu > Cr > Ni > Mn. The PI values for Cd, Pb, and Zn ranged from 0.08 to 68.9, 1.12 to
225 19.5, and 2.77 to 22.8, respectively, with mean values of 16.7, 4.11, and 6.16. For Cd, Pb, and Zn, 96.0%,
226 77.4% and 99.2% of all samples contained considerable pollution levels or greater (PI > 3), indicating
227 that the road dust of Shenyang was seriously contaminated with Cd, Pb, and Zn. I_{geo} and PI results
228 indicated that Cd, Pb, and Zn were the main contaminants in the urban road dust of Shenyang, which
229 may originate from traffic-related exhaust sources (tire, brake and asphalt wear and abrasion) and
230 industrial emissions (Men et al. 2018b; Gope et al. 2018). These results also indicate that I_{geo} and PI can
231 feasibly be used to evaluate heavy metal pollution levels in road dust.

232 As shown in Fig. 2c and Table S3, the PLI values of all dust samples ranged from 1.25 to 5.73, with
233 an average of 3.33, indicating a high pollution level in the urban road dust of Shenyang. There were only
234 four samples (3.23% of all samples) with PLI values below 2, while 94.4% (117 samples) had PLI values
235 between 2 and 5, and 2.42% (3 samples) had PLI values above 5. Overall, these findings suggested that
236 the study area exhibited almost entirely high pollution levels with the urban road dust of Shenyang being
237 seriously polluted by anthropogenic activities.



238
239

240
241

Fig. 2. a) Geo-accumulation index (I_{geo}); b) Pollution index (PI); and c) Pollution load index (PLI) for

242 heavy metals in urban road dust from Shenyang (China).

243 3.3 Source identification

244 Correlations between heavy metals can reflect their sources and pathways (Yang et al., 2011; Lu et
245 al., 2017a). Pearson correlation analysis results are shown in Table 2. Except for an extremely negative
246 correlation with Ni ($p < 0.01$), Cd had no significant correlations with any other heavy metals. Positive
247 correlations ($P < 0.01$) were found between several element pairs: Cr–Mn ($r=0.378$), Cr–Ni ($r=0.369$),
248 Cu–Ni ($r=0.254$), Cu–Pb ($r=0.272$), Cu–Zn ($r=0.488$), Zn–Mn ($r=0.277$), Zn–Ni ($r=0.254$), and Zn–Pb
249 ($r=0.334$). Three element pairs, Cr–Cu ($r=0.189$), Cr–Zn ($r=0.205$) and Cu–Mn ($r=0.214$), exhibited a
250 significantly positive correlation ($P < 0.05$). Similarly, Gope et al. (2018) identified a positive correlation
251 between Cr–Mn, Cr–Ni, Cu–Pb, Cu–Zn, and Pb–Zn in the street dust of Durgapur, India, while Li et al.,
252 (2013) reported a positive correlation between Cr–Mn, Cu–Pb, Cu–Zn, Zn–Mn, and Pb–Zn in urban soil
253 from Shenyang, China. According to previous studies, Cr, Cu, Mn, and Zn are commonly positively
254 correlated, indicating that industrial emissions might be the source, such as steel and alloy processing
255 and thermal power plants (Mousavian et al., 2017; Dietrich et al., 2018). Similarly, a positive correlation
256 was found between Pb and Zn, which might be related to traffic activities (Gope et al., 2018). Cr and Ni
257 are commonly found to be highly correlated in road dust, potentially deriving from a mixture of natural
258 (weathering of soils and pavement) (Yan et al., 2018) and anthropogenic (abrasion of alloys used in-
259 vehicle components and thermal power plants) sources (Chen et al., 2014; Usmani and Kumar 2017).
260 Therefore, the sources of heavy metals in road dust are complex and inconclusive, with the results of
261 correlation analysis not able to identify a dominant source. Therefore, other multivariate statistical
262 analyses were carried out to further explore the relationship between these heavy metals and their sources.

263 **Table 2** Pearson's correlations matrix for metal concentrations in urban road dust from Shenyang (China).

	Cd	Cr	Cu	Mn	Ni	Pb	Zn
Cd	1	-0.14	-0.085	0.055	-0.410**	-0.064	-0.098
Cr		1	0.189*	0.378**	0.369**	0.09	0.205*
Cu			1	0.214*	0.254**	0.272**	0.488**
Mn				1	0.071	-0.002	0.277**
Ni					1	0.137	0.254**
Pb						1	0.334**
Zn							1

264 *. Correlation significant at the 0.05 level (2-tailed).

265 **. Correlation significant at the 0.01 level (2-tailed).

266 Principal component analysis (PCA) was used to study the established correlations, with the aim of
267 providing information on the distribution and sources of heavy metal pollutants. The PCA results indicate
268 that there were three components with eigenvalues > 1 , which explained 67.33% of the total variance
269 (Table 3). PC1 was loaded primarily with Cu, Pb, and Zn, accounting for 24.81% of the total variance.
270 Cu, Pb, and Zn are mainly associated with vehicle exhaust emissions (Pan et al., 2017; Gope et al., 2018).
271 The Cu content of road dust may come from engine and brake wear, as well as mechanical abrasion of
272 vehicle parts, while Zn mainly originates from lubricating oil and attrition of automobile tires (Dehghani
273 et al, 2017). Historically, Pb has been an important gasoline additive and although China banned the
274 addition of Pb to gasoline since the early 2000's, Pb has a long half-life and a low leaching rate, leading
275 to its accumulation in urban environments over time (Yang et al., 2011). It has also been reported that

276 Cu, Pb, and Zn are related to industrial activities as they can be released during metal processing and
 277 smelting (Dietrich et al., 2018). Therefore, PC1 was mainly related to traffic and industrial activities.

278 PC2 explained 21.43% of the total variance and was heavily loaded with Cd and Ni. As shown in
 279 Table 2, Cd (-0.841) exhibited an inverse loading trend compared to Ni (0.787), indicating distinct
 280 sources for Cd and Ni. Based on the metal concentrations and pollution indices, Ni originated from mixed
 281 natural and anthropogenic sources, with emissions from steel and alloy industries, corrosion of vehicle
 282 body parts and abrasion of asphalt pavements being the main sources for Ni accumulation (Dehghani et
 283 al, 2017; Li et al., 2017; Lu et al, 2017a; Gope et al, 2018). In contrast, the sources of Cd were more
 284 complex. Cd is widely used to shelter alloy surfaces and building materials, as well as in electroplating,
 285 and the production of batteries, plastics and fertilizers (Yıldırım and Tokaloğlu., 2016). In recent years,
 286 there have been a large number of urban constructions in Shenyang, including commercial and residential
 287 buildings, a subway, and road widening schemes. As a consequence, traffic sources (lubricating oil and
 288 tire wear) (Men et al., 2018b), industrial sources (thermal power plants and steel) (Gope et al., 2018),
 289 building materials (commercial and residential buildings, road and subway) (Wei et al., 2010) and
 290 agricultural sources (fertilizers and pesticides) (Li et al., 2017), are all potential sources of Cd in the road
 291 dust of Shenyang.

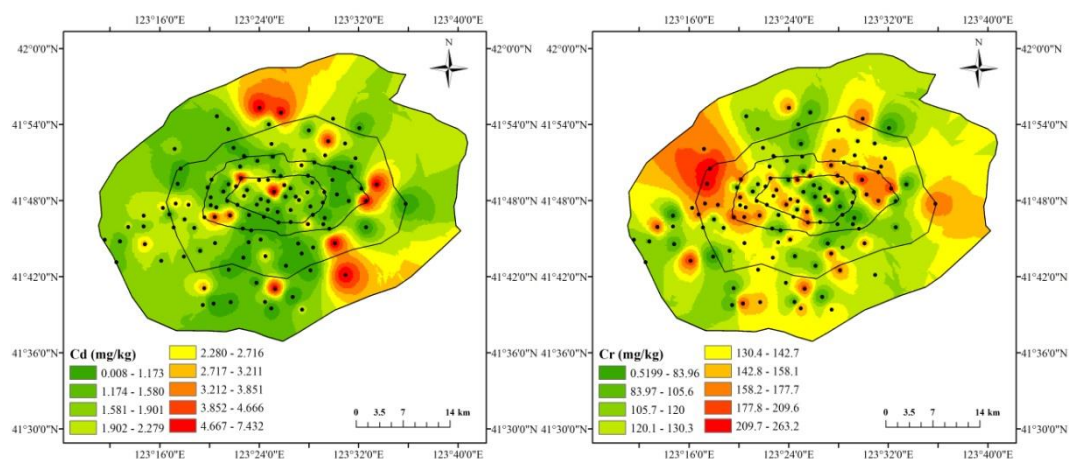
292 The third principal component (PC3) explained 21.10% of the total variance and was heavily loaded
 293 with Cr and Mn. According to the results of statistical analysis and previous studies, Cr and Mn are likely
 294 to originate from mixed sources, mostly from the weathering of parent materials, with a smaller
 295 contribution from industrial emissions. Fly ash produced by burning coal might be a main factor causing
 296 the accumulation of Cr and Mn in road dust (Raja et al., 2014; Wang et al., 2016). Moreover, emissions
 297 from the smelting industry present another anthropogenic source for these two metals (Men et al., 2018b).
 298 **Table 3** Rotated principal component matrix for heavy metals in the urban road dust of Shenyang (PCA
 299 loadings >0.5 are shown in bold).

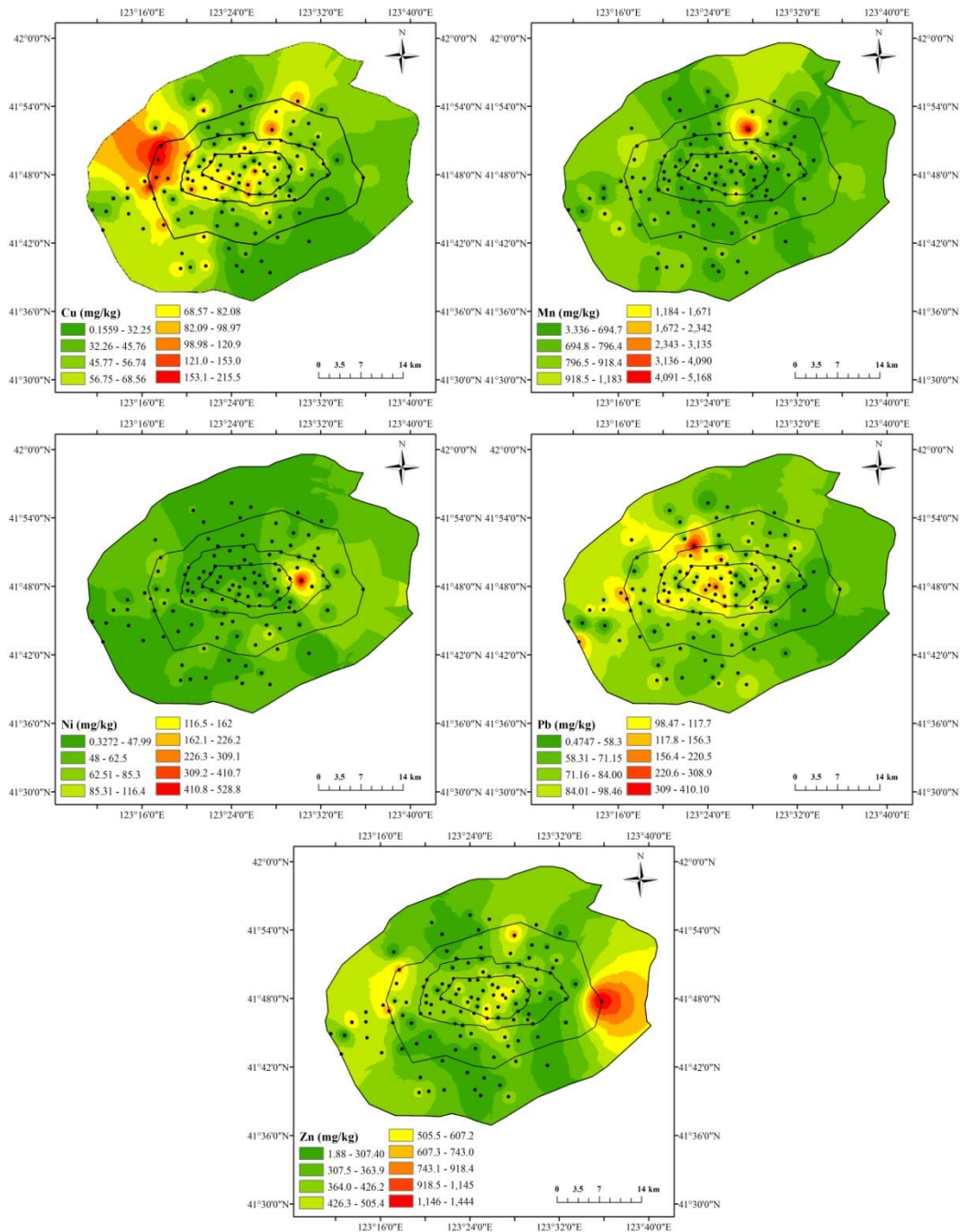
Element	Component		
	PC1		PC1
Cd	-0.014	Cd	-0.014
Cr	0.065	Cr	0.065
Cu	0.730	Cu	0.730
Mn	0.131	Mn	0.131
Ni	0.202	Ni	0.202
Pb	0.746	Pb	0.746
Zn	0.765	Zn	0.765
Eigenvalue	2.294	Eigenvalue	2.294
Total variance (%)	24.81	Total variance (%)	24.81
Cumulative variance (%)	24.81	Cumulative variance (%)	24.81

300 3.4 Spatial distribution

301 Spatial distribution analysis is a useful method for determining the hotspots of elevated heavy metal
 302 concentrations and to identify the potential sources. The estimated maps of Cd, Cr, Cu, Mn, Ni, Pb, and
 303 Zn pollution are presented in Fig. 3, showing that the concentrations of heavy metals in road dust
 304 exhibited a high level of spatial variation. The Cd hotspots had relatively high spatial variability, indicating

305 that the sources of Cd were complex, mainly concentrated in industrial, urban, and suburban areas.
 306 Industrial emissions (thermal power plants, Fe and steel industries) (Verma et al., 2015; Mousavian et al.,
 307 2017), vehicular emission (brake wear, tire wear, and engine oil) (Dehghani et al., 2017), and the
 308 application of pesticides (Cui et al., 2018), may be the major sources for Cd accumulated in road dust.
 309 Among these metals, Cr, Cu, Mn, and Zn exhibited similar spatial distribution patterns, indicating that
 310 these metals may have the same sources. The hotspots of Cr, Cu, Mn, and Zn were found to be located
 311 in the Tiexi industrial district, which might be related to several industrial emission sources. As essential
 312 metals in various metal processing activities, Cr, Cu, Mn, and Zn are widely used to control redox
 313 reactions and improve the strength and hardness of steel and alloys (Gong et al., 2014; Dietrich et al.,
 314 2018). Historically, the Tiexi industrial district has been one of the largest heavy industry zones in China,
 315 with the smelting industry in this region being the backbone of China's metallurgical industry (Li et al.,
 316 2013). As of the end of 2019, there were more than 100 large scale Fe and steel smelting enterprises in
 317 Shenyang (SSB, 2020), which may be a main reason for the accumulation of Cr, Cu, Mn, and Zn in road
 318 dust in this region. Furthermore, some hotspots identified pollution point sources, which might be related
 319 to the steel and non-ferrous metal markets in the north of the study area and the cement plants in the east
 320 (Ogunkunle and Fatoba, 2014). The spatial distribution of Ni pollution was relatively even, with the only
 321 hotspot area located in the mid-east of the city, which might be associated with engine manufacturers
 322 located nearby. Ni-based alloys are widely used in modern engines due to their outstanding performance
 323 in harsh environments, accounting for 40-60% of the total weight of engine materials (Ding et al., 2018).
 324 Therefore, the spatial distribution of Ni might be influenced by soil parent materials and industrial
 325 emissions. The Pb hotspot areas were found to be mainly located within the second ring road area, which
 326 is the political, economic, and cultural center of Shenyang with a high traffic volume, indicating that
 327 vehicular-related activities significantly contribute to Pb accumulation in road dust. In China, although
 328 petrol with Pb additives was banned two decades ago, Pb concentrations in urban soil still reflect the
 329 significant degree of historical Pb contamination and the long half-life of Pb (Yang et al., 2011).
 330 Moreover, Pb can accumulate in urban road dust from soil via resuspension (Chen et al., 2014). However,
 331 vehicular sources (i.e., vehicles using leaded petrol) are still the main sources of atmospheric Pb, leading
 332 to the increase in Pb concentrations in urban road dust.





337 **Fig. 3.** Spatial distribution of heavy metal concentrations in urban road dust from Shenyang.

338 **3.5 Health risk assessment**

339 The non-carcinogenic and carcinogenic risks presented by heavy metals in road dust are shown in
 340 Table S4. For non-carcinogenic effects, the health risks for children were higher than for adults. Children
 341 are more susceptible to the effects of heavy metals, due to children’s behavioral and physiological
 342 characteristics, including hand-to-mouth activities and higher breathing rate per unit body weight (Liu et
 343 al., 2018). The total HI values of multiple metals for adults and children were 0.24 and 1.64, respectively,
 344 indicating that children could suffer from non-carcinogenic effects of multiple heavy metal exposure.
 345 The HQ values for children were < 1 for all the assessed metals, which were ranked in the descending
 346 order of Cr > Pb > Mn > Cu > Ni > Cd > Zn. Although the children’s HQ value for Cr (0.68) was below
 347 the safety threshold, if children are exposed to a sufficiently large dose over a long term period, it may

348 cause neurological and developmental disorders. Therefore, exposure of Cr in urban dust in Shenyang
349 could pose a potential threat to children's health. The contribution from the ingestion pathway was the
350 highest (88.4% for children and 66.8% for adults), followed by dermal contact and inhalation, which is
351 consistent with the reported results of earlier studies (Chabukdhara and Nema, 2013; Tang et al., 2017).

352 Due to the lack of corresponding RfD or SF values, only Cd, Cr, and Ni were evaluated in terms of
353 their carcinogenic risk. Cd exposure was evaluated for all three pathways, while Cr and Ni were only
354 evaluated for carcinogenic health risks via the inhalation pathway. CR values for multiple metal exposure
355 for adults and children were 2.17×10^{-5} and 1.65×10^{-4} , respectively (Table S4). The carcinogenic risk
356 for children was higher than the maximum tolerable value (1×10^{-4}), while the carcinogenic risk for
357 adults was within the acceptable range (1×10^{-6} - 1×10^{-4}). For adults and children, the CR values for Ni
358 were below the negligible risk level of 1×10^{-6} , indicating no significant effect on health. The carcinogenic
359 risk levels for Cr for adults and children and Cd for adults were within the acceptable limits, while the
360 CR values for Cd for children were 1.59-fold higher than the CR threshold. The ingestion pathway
361 accounted for 93.1% and 96.4% of the total CR for adults and children, respectively, which was much
362 higher than the other two pathways, indicating that ingestion was the main CR exposure pathway for
363 both adults and children. Therefore, the non-carcinogenic and carcinogenic risks to children in the study
364 area were higher than the risk to adults, highlighting the need for more research attention in this field and
365 the development of effective mitigation measures.

366 367 **4 Conclusions**

368 The present study determined the concentrations, pollution level, spatial distribution, and health
369 risks of Cd, Cr, Cu, Mn, Ni, Pb, and Zn in urban road dust from Shenyang, Northeast China. The mean
370 concentrations of Cd, Cr, Cu, Mn, Ni, Pb, and Zn in road dust samples were significantly higher than the
371 corresponding soil background values, with Cd, Pb, and Zn being the main polluting metals as indicated
372 by I_{geo} and PI values ranging from moderate to heavy/high contamination levels. Based on PLI values,
373 almost all the study areas were highly polluted. PCA results showed that Cu, Pb, and Zn mainly
374 originated from traffic and industrial sources; Cr, Mn, and Ni had mixed industrial and natural sources;
375 and Cd had a complex source profile related to industrial emissions, vehicular exhaust emissions,
376 building materials, and agricultural activities. GIS mapping further revealed the locations of heavily
377 polluted hotspots for the seven assessed metals. The hotspots of Cr, Cu, Mn, and Zn exhibited similar
378 distribution patterns, which were mainly distributed in the Tiexi district and associated with industrial
379 activities. The spatial distributions of Cd, Ni, and Pb were different from the other metals. Industrial
380 emissions, vehicular emissions, and agricultural activities may be the factors affecting the distribution of
381 Cd hotspots, high traffic density and historical leaded petrol residues were the main factors influencing
382 Pb hotspots, while the spatial distribution of Ni was relatively homogeneous, with only one hotspot area
383 potentially associated with manufacturing emissions. Although exposure to individual metals in urban
384 road dust exhibited a relatively low health risk, the non-carcinogenic risks associated with exposure
385 multiple metals in children exceeded the acceptable level, indicating that children might experience non-
386 carcinogenic effects. The carcinogenic risks of exposure to Cr by both children and adults and Cd by
387 adults were within the acceptable range, while exposure to Cd by children presented an unacceptable
388 risk. Finally, ingestion was found to be the primary exposure pathway for non-carcinogenic and
389 carcinogenic risks for adults and children.

390 391 **Acknowledgments**

392 This research was funded by the Strategic Priority Research Program of the Chinese Academy of
393 Sciences, Grant No. XDA23070502; Natural Science Foundation of Jilin Province, Grant
394 No.20190103161JH.

395 The authors would like to thank all the laboratory persons as well as colleagues for providing their
396 help during sampling and analysis. The authors appreciate the reviewers and editors for their assistance
397 in the development and improvement of this paper.

398

399 Reference

400 Ali M U, Liu G, Yousaf B, Abbas Q, Ullah H, Munir M, Fu B (2017). Pollution characteristics and human
401 health risks of potentially (eco)toxic elements (PTEs) in road dust from metropolitan area of
402 Hefei, China. *Chemosphere*, 181:111–121. <https://doi.org/10.1016/j.chemosphere.2017.04.061>

403 Amjadian K, Pirouei M, Rastegari Mehr M, Shakeri A, Khurshid Rasool S, Ibrahim Haji D (2018).
404 Contamination, health risk, mineralogical and morphological status of street dusts- case study:
405 Erbil metropolis, Kurdistan Region-Iraq. *Environmental pollution (Barking, Essex : 1987)*,
406 243(Pt B):1568–1578. <https://doi.org/10.1016/j.envpol.2018.09.116>

407 Anh H Q, Watanabe I, Tomioka K, Minh T B, Takahashi S (2019). Characterization of 209
408 polychlorinated biphenyls in street dust from northern Vietnam: Contamination status, potential
409 sources, and risk assessment. *The Science of the total environment*, 652:345–355.
410 <https://doi.org/10.1016/j.scitotenv.2018.10.240>

411 Bi C, Zhou Y, Chen Z, Jia J, Bao X (2018). Heavy metals and lead isotopes in soils, road dust and leafy
412 vegetables and health risks via vegetable consumption in the industrial areas of Shanghai, China.
413 *Science of the Total Environment* 619-620:1349-1357.
414 <https://doi.org/10.1016/j.scitotenv.2017.11.177>.

415 Cai Q, Mo C, Li H, Lü H, Zeng Q, Li Y, Wu X (2013). Heavy metal contamination of urban soils and
416 dusts in Guangzhou, South China. *Environmental Monitoring and Assessment* 185(2):1095-
417 1106. <https://doi.org/10.1007/s10661-012-2617-x>.

418 Chabukdhara M, Nema AK (2013). Heavy metals assessment in urban soil around industrial clusters in
419 Ghaziabad, India: probabilistic health risk approach. *Ecotoxicology and Environmental Safety*
420 87(1):57-64. <https://doi.org/10.1016/j.ecoenv.2012.08.032>.

421 Chen H, Teng Y, Lu S, Wang Y, Wang J (2015). Contamination features and health risk of soil heavy
422 metals in China. *Science of The Total Environment* 512-513:143-153.
423 <https://doi.org/10.1016/j.scitotenv.2015.01.025>

424 Chen H., Lu X, Li LY, Gao T, Chang Y (2014). Metal contamination in campus dust of Xi'An, China: a
425 study based on multivariate statistics and spatial distribution. *Science of the Total Environment*
426 484:27-35. <https://doi.org/10.1016/j.scitotenv.2014.03.026>.

427 CNEMC (Chinese National Environmental Monitoring Center) (1990). *The Soil Background Value in*
428 *China*. China Environmental Science Press, Beijing. (in Chinese)

429 Cui Z, Wang Y, Zhao N, Yu R, Xu G, Yu Y (2018). Spatial distribution and risk assessment of heavy
430 metals in paddy soils of Yongshuyu irrigation area from songhua river basin, Northeast China.
431 *Chinese Geographical Science* 28(5):797-809. <https://doi.org/10.1007/s11769-018-0991-1>.

432 Dao L, Morrison L, Zhang C (2010). Spatial variation of urban soil geochemistry in a roadside sports
433 ground in Galway, Ireland. *Science of Total Environment* 408:1076-1084.
434 <https://doi.org/10.1016/j.scitotenv.2009.11.022>.

435 Dehghani S, Moore F, Keshavarzi B, Hale BA (2017). Health risk implications of potentially toxic metals

436 in street dust and surface soil of Tehran, Iran. *Ecotoxicology and Environmental Safety* 136:92-
437 103. <https://doi.org/10.1016/j.ecoenv.2016.10.037>.

438 Dietrich M, Huling J, Krekeler MPS (2018). Metal pollution investigation of Goldman Park, Middletown
439 Ohio: Evidence for steel and coal pollution in a high child use setting. *Science of The Total*
440 *Environment* 618:1350-1362. <https://doi.org/10.1016/j.scitotenv.2017.09.246>.

441 Ding W, Miao Q, Li B, Xu J (2018). Review on Grinding Technology of Nickel-based Superalloys Used
442 for Aero-engine. *Journal of Mechanical Engineering* 55(01):189-215. (in Chinese)

443 Du Y, Gao B, Zhou H, Ju X, Hao H, Yin S (2013). Health risk assessment of heavy metals in road dusts
444 in urban parks of Beijing, China. *Procedia Environmental Sciences* 18:299-309.
445 <https://doi.org/10.1016/j.proenv.2013.04.039>.

446 Gong X, Chen Z, Luo Z (2014). Spatial distribution, temporal variation, and sources of heavy metal
447 pollution in groundwater of a century-old nonferrous metal mining and smelting area in China.
448 *Environmental Monitoring and Assessment* 186(12):9101-9116.
449 <https://doi.org/10.1007/s10661-014-4069-y>.

450 Gope M, Masto RE, George J, Balachandran S (2018). Tracing source, distribution and health risk of
451 potentially harmful elements (PHEs) in street dust of Durgapur, India. *Ecotoxicology and*
452 *Environmental Safety* 154:280-293. <https://doi.org/10.1016/j.ecoenv.2018.02.042>.

453 Gope M, Masto RE, George J, Hoque RR, Balachandran S (2017). Bioavailability and health risk of
454 some potentially toxic elements (Cd, Cu, Pb and Zn) in street dust of Asansol, India.
455 *Ecotoxicology and Environmental Safety* 138:231-241.
456 <https://doi.org/10.1016/j.ecoenv.2017.01.008>.

457 Hu B, Liu B, Zhou J, Guo J, Sun Z, Meng W, Guo X, Duan J (2016). Health risk assessment on heavy
458 metals in urban street dust of tianjin based on trapezoidal fuzzy numbers. *Human and Ecological*
459 *Risk Assessment: An International Journal* 22(3):678-692.
460 <https://doi.org/10.1080/10807039.2015.1104625>.

461 Jiao X, Teng Y, Zhan Y, Wu J, Lin X (2015). Soil heavy metal pollution and risk assessment in shenyang
462 industrial district, northeast china. *PLOS ONE* 10(5):e0127736.
463 <https://doi.org/10.1371/journal.pone.0127736>.

464 Khademi H, Gabarrón M, Abbaspour A, Martínez-Martínez S, Faz A, Acosta JA (2019). Environmental
465 impact assessment of industrial activities on heavy metals distribution in street dust and soil.
466 *Chemosphere* 217:695-705. <https://doi.org/10.1016/j.chemosphere.2018.11.045>.

467 Khanal R, Furumai H, Nakajima F, Yoshimura C (2018). Carcinogenic profile, toxicity and source
468 apportionment of polycyclic aromatic hydrocarbons accumulated from urban road dust in Tokyo,
469 Japan. *Ecotoxicology and environmental safety*, 165:440–449.
470 <https://doi.org/10.1016/j.ecoenv.2018.08.095>

471 Lanzerstorfer C (2018). Heavy metals in the finest size fractions of road-deposited sediments.
472 *Environmental Pollution* 239:522-531. <https://doi.org/10.1016/j.envpol.2018.04.063>.

473 Li H, Chen L, Yu L, Guo Z, Shan C, Lin J, Gu Y, Yang Z, Yang Y, Shao J, Zhu X, Cheng Z (2017).
474 Pollution characteristics and risk assessment of human exposure to oral bioaccessibility of
475 heavy metals via urban street dusts from different functional areas in Chengdu, China. *Science*
476 *of The Total Environment* 586:1076-1084. <https://doi.org/10.1016/j.scitotenv.2017.02.092>.

477 Li X, Liu L, Wang Y, Luo G, Chen X, Yang X, Hall Myrna, Guo R, Wang H, Cui J, He X (2013). Heavy
478 metal contamination of urban soil in an old industrial city (Shenyang) in Northeast China.
479 *Geoderma* 192:50-58. <https://doi.org/10.1016/j.geoderma.2012.08.011>.

480 Liang L, An L, Yang L, Zhang L, Zhang G, Guan Y (2016). Polycyclic aromatic hydrocarbons associated
481 with road deposited solid and their ecological risk: implications for road stormwater reuse.
482 Science of the Total Environment 563-564:190-198.
483 <https://doi.org/10.1016/j.scitotenv.2016.04.114>.

484 Liu E, Yan T, Birch Gavin, Zhu Y (2014). Pollution and health risk of potentially toxic metals in urban
485 road dust in Nanjing, a mega-city of China. Science of the Total Environment 476-477:522-531.
486 <https://doi.org/10.1016/j.scitotenv.2014.01.055>.

487 Liu L, Cui Z, Wang Y, Rui Y, Yang Y, Xiao Y (2018). Contamination features and health risk of heavy
488 metals in suburban vegetable soils, Yanbian, Northeast China. Human & Ecological Risk
489 Assessment. 1-16. <https://doi.org/10.1080/10807039.2018.1450135>.

490 Lu X, Pan H, Wang Y (2017a). Pollution evaluation and source analysis of heavy metal in roadway dust
491 from a resource-typed industrial city in Northwest China. Atmospheric Pollution Research
492 8(3):587-595. <https://doi.org/10.1016/j.apr.2016.12.019>.

493 Lu X, Shi D, Yin N, Pan H, Smith Paris (2017b). Risk assessment of heavy metals in finer than 63- μ m
494 dust particles from various functional areas in Xi'an, China. Air Quality, Atmosphere & Health
495 10(7):907-915. <https://doi.org/10.1007/s11869-017-0480-1>.

496 Lu X, Wang L, L LY, Lei K, Huang L, Kang D (2010). Multivariate statistical analysis of heavy metals
497 in street dust of Baoji, NW China. Journal of Hazardous Materials 173(1-3):744-749.
498 <https://doi.org/10.1016/j.jhazmat.2009.09.001>.

499 Maanan M, Saddik M, Maanan M, Chaibi M, Assobhei O, Zourarah B (2015). Environmental and
500 ecological risk assessment of heavy metals in sediments of Nador lagoon, Morocco. Ecological
501 Indicators 48:616-626. <https://doi.org/10.1016/j.ecolind.2014.09.034>.

502 Mathur R, Balaram V, Satyanarayanan M, Sawant SS (2016). Assessment of heavy metal contamination
503 of road dusts from industrial areas of Hyderabad, India. Environmental Monitoring &
504 Assessment 188(9):514. <https://doi.org/10.1007/s10661-016-5496-8>.

505 Men C, Liu R, Wang Q, Guo L, Shen Z (2018a). The impact of seasonal varied human activity on
506 characteristics and sources of heavy metals in metropolitan road dusts. Science of the Total
507 Environment 637: 844-854. <https://doi.org/10.1016/j.scitotenv.2018.05.059>.

508 Men C, Liu R, Xu F, Wang Q, Guo L, Shen Z (2018b). Pollution characteristics, risk assessment, and
509 source apportionment of heavy metals in road dust in Beijing, China. Science of The Total
510 Environment 612:138-147. <https://doi.org/10.1016/j.scitotenv.2017.08.123>.

511 Mousavian N A, Mansouri N, Nezhadkurki F (2017). Estimation of heavy metal exposure in workplace
512 and health risk exposure assessment in steel industries in Iran. Measurement 102:286-290.
513 <https://doi.org/10.1016/j.measurement.2017.02.015>.

514 Ogunkunle C O, Fatoba P O (2014). Contamination and spatial distribution of heavy metals in topsoil
515 surrounding a mega cement factory. Atmospheric Pollution Research 5(2):270-282.
516 <https://doi.org/10.5094/APR.2014.033>.

517 Pan H, Lu X, Lei K (2017). A comprehensive analysis of heavy metals in urban road dust of Xi'an, China:
518 Contamination, source apportionment and spatial distribution. Science of the Total Environment
519 609:1361-1369. <https://doi.org/10.1016/j.scitotenv.2017.08.004>.

520 Raja R, Nayak AK, Rao KS, Puree C, Shahid M, Panda BB, Kumar A, Tripathi R, Bhattacharyya P, Baig
521 MJ, Lal B, Mohanty S, Gautam P (2014). Effect of fly ash deposition on photosynthesis, growth
522 and yield of Rice. Bulletin of Environmental Contamination and Toxicology 93:106-112.
523 <https://doi.org/10.1007/s00128-014-1282-x>.

524 Salo H, Paturi P, Mkinen J (2016). Moss bag (*sphagnum papillosum*) magnetic and elemental properties
525 for characterising seasonal and spatial variation in urban pollution. *International journal of*
526 *Environmental Science and Technology* 13(6):1515-1524. [https://doi.org/10.1007/s13762-016-](https://doi.org/10.1007/s13762-016-0998-z)
527 [0998-z](https://doi.org/10.1007/s13762-016-0998-z).

528 SEPA (State Environmental Protection Administration of China) (1997). *Soil Quality-Determination of*
529 *Copper, Zinc-Flame atomic absorption spectrophotometry*. GB/T 17138-1997. Ministry of
530 Environment Protection of the People's Republic of China, Beijing, China. (in Chinese)

531 Shenyang Statistics Bureau (SSB) (2020). *Statistical bulletin of national economic and social*
532 *development of Shenyang in 2019*. <http://tjj.shenyang.gov.cn/systj/tjsj/ndsj/glist.html>.
533 Accessed 31 December 2020 (in Chinese).

534 Shi D, Lu X (2018). Accumulation degree and source apportionment of trace metals in smaller than 63
535 μm road dust from the areas with different land uses: A case study of Xi'an, China. *Science of*
536 *The Total Environment* 636:1211-1218. <https://doi.org/10.1016/j.scitotenv.2018.04.385>.

537 Shi X, Chen L, Wang J (2013). Multivariate analysis of heavy metal pollution in street dusts of Xianyang
538 city, NW China. *Environmental Earth Sciences* 69(6):1973-1979.
539 <https://doi.org/10.1007/s12665-012-2032-1>.

540 Soltani N, Keshavarzi B, Moore F, Tavakol T, Reza Lahijanzadeh A, Jaafarzadeh N, Kermani M (2015).
541 Ecological and human health hazards of heavy metals and polycyclic aromatic hydrocarbons
542 (PAHs) in road dust of Isfahan metropolis, Iran. *Science of the Total Environment* 505:712-723.
543 <https://doi.org/10.1016/j.scitotenv.2014.09.097>.

544 Taiwo AM, Awomeso JA, Taiwo OT, Oremodu BD, Akintunde OO, Ojo NO, Elegbede, OO, Olanrewaju
545 HH, Arowolo TA (2017). Assessment of health risks associated with road dusts in major traffic
546 hotspots in Abeokuta Metropolis, Ogun State, Southwestern Nigeria. *Stochastic Environmental*
547 *Research and Risk Assessment* 31:431-447. <https://doi.org/10.1007/s00477-016-1302-y>.

548 Talbi A, Kerchich Y, Kerbachi R, Boughedaoui M (2017). Assessment of annual air pollution levels with
549 PM 1, PM 2.5, PM 10 and associated heavy metals in Algiers, Algeria. *Environmental Pollution*
550 232:252-263. <https://doi.org/10.1016/j.envpol.2017.09.041>.

551 Tang Z, Chai M, Cheng J, Jin J, Yang Y, Nie Z, Huang Q, Li Y (2017). Contamination and health risks
552 of heavy metals in street dust from a coal-mining city in eastern China. *Ecotoxicology &*
553 *Environmental Safety* 138:83-91. <https://doi.org/10.1016/j.ecoenv.2016.11.003>.

554 Trujillo-González JM, Torres-Mora MA, Keesstra S, Brevik EC, Jiménez-Ballesta R (2016). Heavy
555 metal accumulation related to population density in road dust samples taken from urban sites
556 under different land uses. *Science of Total Environmet* 553:636-642.
557 <https://doi.org/10.1016/j.scitotenv.2016.02.101>.

558 Urrutia-Goyes R, Hernandez N, Carrillo-Gamboa O, Nigam KDP, Ornelas-Soto N (2018). Street dust
559 from a heavily-populated and industrialized city: evaluation of spatial distribution, origins,
560 pollution, ecological risks and human health repercussions. *Ecotoxicology and Environmental*
561 *Safety* 159:198-204. <https://doi.org/10.1016/j.ecoenv.2018.04.054>.

562 USEPA (US Environmental Protection Agency) (1989). *Risk Assessment Guidance for Superfund, Vol.*
563 *I: Human Health Evaluation Manual vol EPA/540/1-89/002*. Office of Soild Waste and Emergency
564 Response, Washington, DC, USA.

565 USEPA (US Environmental Protection Agency) (1997). *Exposure Factors Handbook*. Environmental
566 Protection Agency, Office of Research and Development, Washington, DC, USA.

567 USEPA (US Environmental Protection Agency) (2001). *Supplemental Guidance for Developing Soil*

568 Screening Levels for Superfund Sites vol OSWER 9355.4-24. Office of Solid Waste and
569 Emergency Response, Washington, DC, USA.

570 Usmani Z, Kumar V (2017). Characterization, partitioning, and potential ecological risk quantification
571 of trace elements in coal fly ash. *Environmental Science & Pollution Research* 24(18):1-20.
572 <https://doi.org/10.1007/s11356-017-9171-6>.

573 Verma SK, Masto RE, Gautam S, Choudhury DP, Ram LC, Maiti SK, Maity S (2015). Investigations on
574 PAHs and trace elements in coal and its combustion residues from a power plant. *Fuel* 162:138–
575 147. <https://doi.org/10.1016/j.fuel.2015.09.005>.

576 Wan D, Han Z, Yang J, Yang G, Liu X (2016). Heavy Metal Pollution in Settled Dust Associated with
577 Different Urban Functional Areas in a Heavily Air-Polluted City in North China. *International*
578 *journal of environmental research and public health*, 13(11):1119.
579 <https://doi.org/10.3390/ijerph13111119>

580 Wang J, Li S, Cui X, Li H, Qian X, Wang C, Sun Y (2016). Bioaccessibility, sources and health risk
581 assessment of trace metals in urban park dust in Nanjing, Southeast China. *Ecotoxicology and*
582 *Environmental Safety* 128:161–170. <https://doi.org/10.1016/j.ecoenv.2016.02.020>.

583 Wei B, Jiang F, Li X, Mu S (2010). Heavy metal induced ecological risk in the city of Urumqi, NW China.
584 *Environmental Monitoring & Assessment* 160(1-4):33-45. [https://doi.org/10.1007/s10661-008-](https://doi.org/10.1007/s10661-008-0655-1)
585 [0655-1](https://doi.org/10.1007/s10661-008-0655-1).

586 Wei X, Gao B, Wang P, Zhou H, Lu J (2015). Pollution characteristics and health risk assessment of
587 heavy metals in street dusts from different functional areas in Beijing, China. *Ecotoxicology*
588 *and Environmental Safety* 112:186-192. <https://doi.org/10.1016/j.ecoenv.2014.11.005>.

589 Yan G, Mao L, Liu S, Mao Y, Ye H, Huang T, Li F, Chen L (2018). Enrichment and sources of trace
590 metals in roadside soils in Shanghai, China: A case study of two urban/rural roads. *Science of*
591 *the Total Environment*. s631–632:942-950. <https://doi.org/10.1016/j.scitotenv.2018.02.340>.

592 Yang T, Zeng Q, Liu Z, Liu QS (2011). Magnetic properties of the road dusts from two parks in Wuhan
593 city, China: Implications for mapping urban environment. *Environmental Monitoring and*
594 *Assessment* 177(1–4):637–648. <https://doi.org/10.1007/s10661-010-1662-6>.

595 Yıldırım G, Tokaloğlu Ş (2016). Heavy metal speciation in various grain sizes of industrially
596 contaminated street dust using multivariate statistical analysis. *Ecotoxicology and*
597 *environmental safety*, 124:369–376. <https://doi.org/10.1016/j.ecoenv.2015.11.006>.

Supplementary Files

This is a list of supplementary files associated with this preprint. Click to download.

- [Supportinginformation.docx](#)